

---

# VEC2FACE: SCALING FACE DATASET GENERATION WITH LOOSELY CONSTRAINED VECTORS

Haiyu Wu<sup>1</sup>, Jaskirat Singh<sup>2</sup>, Sicong Tian<sup>3</sup>, Liang Zheng<sup>2</sup>, Kevin W. Bowyer<sup>1</sup>

<sup>1</sup>University of Notre Dame

<sup>2</sup>The Australian National University

<sup>3</sup>Indiana University South Bend

{hwu6@nd.edu, jaskirat.singh@anu.edu, tiansic@iu.edu}

{liang.zheng@anu.edu, kwb@nd.edu}

## ABSTRACT

This paper studies how to synthesize face images of non-existent persons, to create a dataset that allows effective training of face recognition (FR) models. Two important goals are (1) the ability to generate a large number of distinct identities (inter-class separation) with (2) a wide variation in appearance of each identity (intra-class variation). However, existing works 1) are typically limited in how many well-separated identities can be generated and 2) either neglect or use a separate editing model for attribute augmentation. We propose Vec2Face, a holistic model that uses only a sampled vector as input and can flexibly generate and control face images and their attributes. Composed of a feature masked autoencoder and a decoder, Vec2Face is supervised by face image reconstruction and can be conveniently used in inference. Using vectors with low similarity among themselves as inputs, Vec2Face generates well-separated identities. Randomly perturbing an input identity vector within a small range allows Vec2Face to generate faces of the same identity with robust variation in face attributes. It is also possible to generate images with designated attributes by adjusting vector values with a gradient descent method. Vec2Face has efficiently synthesized as many as 300K identities with 15 million total images, whereas 60K is the largest number of identities created in the previous works. FR models trained with the generated HSFace datasets, from 10k to 300k identities, achieve state-of-the-art accuracy, from 92% to 93.52%, on five real-world test sets. For the first time, our model created using a synthetic training set achieves higher accuracy than the model created using a same-scale training set of real face images (on the CALFW test set). Code link: <https://haiyuwu.github.io/vec2face.github.io/>

## 1 INTRODUCTION

We aim to synthesize face images in a way that enables large-scale training sets for FR models, which have the potential to address privacy issues arising with web-scraped datasets of real face images. It is generally recognized that a good training set for FR should have high inter-class separability (Kim et al., 2023; Boutros et al., 2023a) and intra-class variation (Qiu et al., 2021; Boutros et al., 2022a; Kim et al., 2023; Boutros et al., 2023a).

However, existing methods lack flexibility in controlling the generation process, leading to unsatisfactory inter-class and intra-class results. On the one hand, Boutros et al. (2023a) point out that identities generated in (Qiu et al., 2021; Boutros et al., 2022b;a; 2024) have relatively low separability because identity generation is controlled by either a single coefficient or by hard class labels. On the other hand, while it is useful to employ identity features as a condition to increase inter-class separability (Boutros et al., 2023a; Papantoniou et al., 2024), it is non-trivial to increase intra-class variation without the use of a separate model such as ControlNet (Zhang et al., 2023) or a model for style transfer.

In light of the above, this paper proposes Vec2Face, a flexible model enabling the generation of large-scale FR datasets. In inference, the workflow of Vec2Face is similar to (Papantoniou et al., 2024; Boutros et al., 2023a), which use a random vector as input and output a face image. But the

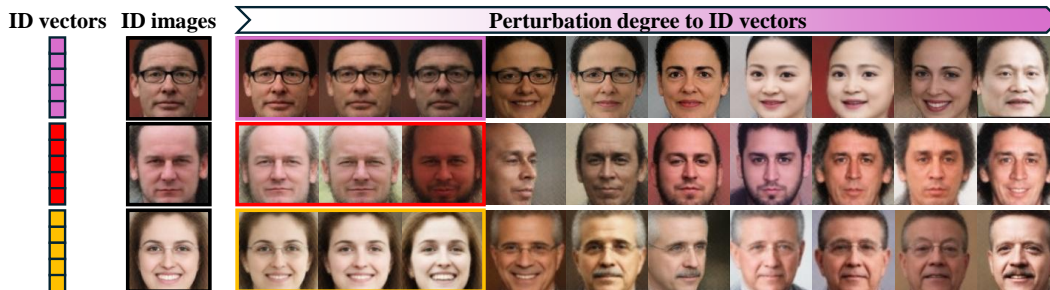


Figure 1: Sample images generated by Vec2Face. From a random vector we generate a face (ID image). We then add random values to this vector to generate diverse face images. Larger perturbation added to this vector results in larger dissimilarity to the ID images. The images in the frame are likely the same person as the ID image.

*interesting* property of Vec2Face is that a small perturbation of the input vector leads to a face image of the same identity but with small changes in appearance, *e.g.*, pose, expression, and facial hair, while a large perturbation of the input vector produces a face image of a different identity (Fig. 1). With this property, and because of the high-dimensionality (*i.e.*, 512-dim) of the input vectors, we can easily 1) sample a large number of identity vectors by controlling their similarity with each other to be under a certain threshold and 2) synthesize a large number of face images by perturbing the identity vectors within a small range. Additionally, we can guide the image content at time of generation using a gradient descent method to efficiently generate faces with minority attributes, such as extreme pose angles.

Using a proper cosine similarity threshold (*i.e.*, 0.3) to sample vectors, the special design of Vec2Face ensures a high ratio of transferring the similarity between vectors to the similarity between generated images, resulting in large inter-class separability; intra-class variation is also properly large because we controlled the variance of the noise for perturbation, so the generated images have  $\geq 0.5$  similarity with the identity vector, exhibiting various appearances while preserving the identity. Experimentally, we verify these inter-class and intra-class variations are beneficial (in hyper-parameter analysis). Because of this, FR models trained on the synthesized 10k identities and 500k images demonstrate very competitive accuracy compared with the state-of-the-art synthetic databases of the same scale (Kim et al., 2023; Papantoniou et al., 2024). Importantly, we show that scaling up the synthetic training data to 10 million images and 200k identities leads to further accuracy improvement. It is also worth noting that results on CALFW (Zheng et al., 2017) represent the first instance where a model trained with synthetic data yields higher accuracy than that trained with real data at the same scale. To our knowledge, this is the first time a synthetic dataset can be this large and more useful.

The training of Vec2Face aims to let a vector generate a face and let its perturbation magnitudes reflect face change magnitudes. To this end, in training we use vectors extracted from real face images by a pre-trained FR model. These vectors are fed into a feature masked autoencoder architecture, after which a decoder produces images similar to the real ones on the pixel level. We summarize the main points of this paper below.

- We propose Vec2Face, a face synthesis model that allows us to efficiently synthesize a large number of face images and identities. Under an appropriate similarity threshold, Vec2Face effectively increases inter-class separability and intra-class variations of synthesized face images.
- With a generated dataset of 10k identities and 500k images, we achieve state-of-the-art FR accuracy measured as the average on five real-world test sets compared with existing synthetic datasets. Our performance even surpasses the accuracy obtained by real training data on one of the five test sets. We also report that scaling to larger synthetic training data leads to further improvement.

## 2 RELATED WORK

**Class conditioned image generation.** VQGAN (Esser et al., 2021), MAGE (Li et al., 2023), DiT (Peebles & Xie, 2023), U-ViT (Bao et al., 2022), MDT (Gao et al., 2023), and VAR (Tian et al., 2024) control the object classes of generated images using discrete class labels as a condition, and so do not support the generation of new classes. Therefore, they are not applicable to scalable

---

face/identity generation. Different from them, Vec2Face uses continuous face features and thus technically can generate an unlimited number of new identities given appropriate feature sampling.

**Feature conditioned image generation.** The models trained with conditioned features, either from a text encoder or an image encoder, perform impressively on diverse class generation. However, (Papantoniou et al., 2024) reports that text embedding exhibits a deficiency in face identity retention. (Chen et al., 2023; Li et al., 2024; Xiao et al., 2023; Wang et al., 2024; Valevski et al., 2023; Ye et al., 2023; Yan et al., 2023; Papantoniou et al., 2024) use an image encoder, either CLIP (Radford et al., 2021) or a FR model, to guide the generation process. These methods are less efficient and effective because 1) the image generation is computationally expensive on these models and 2) they use a fixed vector to generate the images from an identity, which *loses the control over the attribute variation*. We posit that face feature vectors contain both identity and attribute information. To this end, our method learns image generation and achieves output control *purely on face features*.

**Synthetic face image datasets.** Existing approaches are primarily based on two methods: GAN-based models and diffusion models, with the latter generally producing datasets that enable FR models to achieve better accuracy. Here, we briefly summarize some important works.

**GAN-based methods:** SynFace (Qiu et al., 2021), USynthface (Boutros et al., 2022b), SFace (Boutros et al., 2022a), SFace2 (Boutros et al., 2024), and ExfaceGAN (Boutros et al., 2023b) leverage pre-trained GAN models to generate datasets. These methods are less effective because the pre-trained GAN models were *not trained in an identity-aware manner*. Departing from them, our method *explicitly uses face features* in training, so the generated images are identity-aware.

**Diffusion model-based methods:** DCFace (Kim et al., 2023) uses a strong pre-trained diffusion model (Choi et al., 2021) and an additional style-transfer model to increase the identity separability and attribute variation. Again, this pretrained model is also *not identity-aware*. IDiff-Face (Boutros et al., 2023a) combines the pretrained encoder and decoder from VQGAN (Esser et al., 2021) with a latent diffusion model conditioned by identity features to control the separability of the generated identities. Although the latent diffusion model is identity-aware, the pre-trained VQGAN *reduces the sensitivity of identity on the output*. Arc2Face (Papantoniou et al., 2024) fine-tunes a pre-trained stable diffusion model (Rombach et al., 2022) on the WebFace42M dataset to increase the generalizability on face. It combines the identity features and CLIP (Radford et al., 2021) to control the identity of output images. The pose variation is increased by adding an additional ControlNet (Zhang et al., 2023). Neither the pre-trained stable diffusion model nor CLIP are optimized for face and the slow processing speed strongly limits large scale dataset generation. On the contrary, our method is specifically designed for face dataset generation and is both identity-aware and fast in generation. This allows our method to achieve state-of-the-art performance while easily scaling the dataset size to 15M.

## 3 METHOD

### 3.1 VEC2FACE

As shown in Fig. 2, Vec2Face consists of a FR model, a feature Masked Autoencoder, an image decoder, and a patch-based discriminator (Isola et al., 2017; Yu et al., 2022).

**Feature extraction and expansion.** Given a real-world face image, following (Boutros et al., 2023a; Papantoniou et al., 2024), we compute its feature using a FR model. To match the input shape of  $MAE_f$ , the extracted image feature is projected and expanded to a 2-D feature map.

**Feature masked auto-encoder (fMAE).** Similar to MAE (He et al., 2022), the model is forced to learn better information by masking out the input. Different from the MAE that masks an input image and introduce mask tokens to form the full-size image, the fMAE uses a 2D feature map as input and masks this feature map. To provide more useful information, the image feature is used to form the full-size feature map. Specifically, the rows in the feature map are randomly masked out by  $x\%$  before the encoding process, where  $x\% \in \mathcal{N}_{truncated}(max = 1, min = 0.5, mean = 0.75)$ , and the image feature is filled in the masked out positions to form the full-size feature map before being processed by the decoder. The structure is in the Appendix.

**Image Decoder.** Finally, the new feature map is passed through a simple image decoder to generate/reconstruct the images. To improve image quality, a patch-based discriminator is integrated to form a GAN-type training.

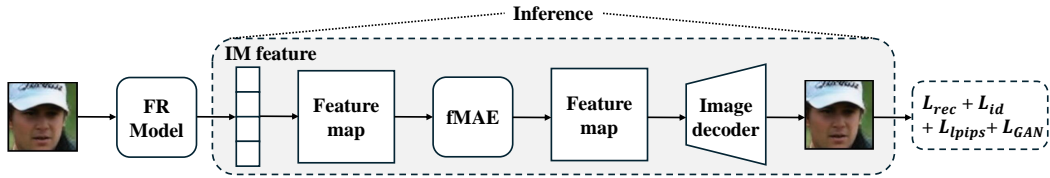


Figure 2: Architecture of Vec2Face. Given a real face image, we compute its feature “IM feature” using a face recognition (FR) model. The feature is expanded into a feature map, and the latter is processed by a feature masked auto-encoder (fMAE). Inside the fMAE, the rows in the feature map are randomly masked out before being processed by the encoder. The image features are then introduced to form the full-size feature map before being processed by the decoder. Finally, the decoder outputs a feature map. Outside the fMAE, a small image decoder reconstructs the pixels in the original image based on the output of fMAE. During inference, Vec2Face accepts a randomized vector and generates a face image. This process has properties demonstrated in Fig. 1.



Figure 3: Generation results for training (**left**) and unseen (**right**) identities. Images in the same row are of the same identity. We extract features from original images and feed them to Vec2Face. We observe that the reconstructed images still maintain the same identity while removing some image borders and backgrounds and transferring sketches into photo-realistic images.

**Loss function.** The training objective functions include an image reconstruction loss and an identity loss. The reconstruction loss can be written as,

$$L_{rec} = MSE(IM_{rec}, IM_{gt}), \quad (1)$$

which compares the pixel-level difference between the reconstructed image  $IM_{rec}$  and the input ground truth images  $IM_{gt}$ . The identity loss is written as:

$$L_{id} = 1 - CosineSimilarity(FR(IM_{rec}), FR(IM_{gt})), \quad (2)$$

meaning that the features of the reconstructed image and original image extracted using the FR model should be close. In addition, the perceptual loss (Zhang et al., 2018) is used to ensure the correct face structure at the early training stage and a patch-based discriminator (Isola et al., 2017; Yu et al., 2022) is used to form the GAN loss to increase the sharpness of the generated images. The training loss is:

$$L_{total} = L_{rec} + L_{id} + L_{lpips} + L_{GAN}. \quad (3)$$

Without  $L_{id}$ , Vec2Face has slightly degraded generation performance but still works reasonably well on identity preservation. Without  $L_{lpips}$ , the reconstructed images do not have clear face structures. Using  $L_{GAN}$  at early training stages makes the model convergence difficult, so it is used only after 1,000 epochs. Examples of loss effect on image reconstruction are in Appendix.

**Sample generation results.** Image generation results are shown in Fig. 3. For both seen and unseen identities, the generated images have very similar identities to the original images. Moreover, the reconstructed image would remove image border artifacts and some complex backgrounds and translate sketches into photo-realistic images.

### 3.2 SAMPLING IDENTITIES AND FACE IMAGES

For Vec2Face, dissimilar input vectors will likely lead to images of different identities, allowing us to generate different identity images; controlling the perturbed identity vectors in a proper similarity range with the identity vector can generate face images with different attributes while preserving the identity.

**Sampling identity images.** Suppose we want to generate  $n$  identity images from  $n$  identity vectors  $v_1, v_2, \dots, v_n$ , where  $v_i \in \mathbb{R}^d, i = 1, 2, \dots, n$ . We ask that the similarity between any pair of identity vectors be less than a threshold  $\tau$ :  $\text{sim}(v_i, v_j) \leq \tau, \forall i \neq j$ . This ensures that the generated images are of different identities. This paper follows (Papantoniou et al., 2024) in using PCA, without dimension reduction, learned on identity features of MS1MV2 (Deng et al., 2019) to randomly sample vectors. Specifically, we first compute the mean and covariance of the PCA-transformed identity features, then use these statistics to generate new samples in the PCA space via multivariate normal distribution, and finally inverse transform these samples back to the original feature space to obtain new identity vectors. Newly sampled vectors that have similarity  $\leq \tau = 0.3$  with all existing vectors are kept, otherwise they are dropped. Interestingly, we notice that, in the high-dimensional (512 in this paper) feature space, most of the randomly sampled vectors fit the condition due to sparsity. Thus, in practice, only 1.7% of the sampled 300k vectors are filtered out.

**Sampling images for each identity.** After obtaining  $n$  identity vectors  $v_1, v_2, \dots, v_n$ , we sample  $m$  vectors for each identity vector by perturbation:

$$v_{im_k} = v_n + \mathcal{N}(0, \sigma), \quad k = 1, 2, \dots, m, \quad (4)$$

where  $v_{im_k}$  is the  $k$ th vector for an identity,  $k = 1, \dots, m$ .  $\mathcal{N}(0, \sigma)$  is a Gaussian distribution with 0 mean and  $\sigma$  variance. To ensure the identity-consistency after perturbation, the similarity values between perturbed vectors and their identity vectors are  $\geq 0.5$ .

Technically speaking, the above steps allow us to synthesize an unlimited number of identities and images using loosely constrained vectors. Hyperparameter  $\tau$  is selected such that identities are well-separated, *i.e.*, high inter-class variation, although it does not act as a strong filter in practice; the selection of hyperparameter  $\sigma$  should enable the generated images for an identity to have large enough variance while staying on the same identity, *i.e.*, high intra-class variation.

### 3.3 EXPLICIT FACE ATTRIBUTE CONTROL

By default, Vec2Face generates images without explicit attribute control. This might lead to some attributes being under-represented, *e.g.*, too few profile head poses. We introduce attribute operation, or AttrOP, to guide vector perturbation so that additional images of desired attributes can be generated. This work focuses on face pose and image quality.

Inspired by (Singh et al., 2023), AttrOP controls the attributes of the generated images by simply adjusting the values in the feature vectors via gradient descent, a process shown in Algorithm 1. Specifically, we first set a target image quality  $Q$  and pose angle  $P$  and prepare a pretrained pose evaluation model  $M_{pose}$  and a pretrained quality evaluation model  $M_{quality}$ . Then, given an identity vector  $v_{id}$  and a perturbed identity vector  $v_{im}$ , we generate a face image from an adjusted vector  $v'_{im}$  and compute the following loss functions:

$$\begin{aligned} \mathcal{L}_{attrop} &= \mathcal{L}_{id} + \mathcal{L}_{quality} + \mathcal{L}_{pose} \text{ where,} \\ \mathcal{L}_{id} &= 1 - \text{CosSim}(M_{FR}(IM), v_{id}), \\ \mathcal{L}_{quality} &= Q - M_{quality}(IM), \\ \mathcal{L}_{pose} &= \text{abs}(P - \text{abs}(M_{pose}(IM))), \end{aligned} \quad (5)$$

Because both  $M_{pose}$  and  $M_{quality}$  are differentiable, gradient descent can be used to adjust  $v'_{im}$  to minimize  $\mathcal{L}_{attrop}$ . We finally use the adjusted  $v'_{im}$  to generate images that exhibit the desired pose and image quality. Sample images optimized by AttrOP are shown in Fig. 4, where profile poses and various image quality levels can be seen.

### 3.4 DISCUSSION

**Novelty statement.** Generating large-scale training sets presents high demands on inter-class separability and intra-class variation. Controlling the identity by either a coefficient or hard class labels is not effective. Conditioning on identity vectors or clustering generated images with a FR model could effectively generate well-separated identities but needs an additional model to address the shortage of intra-class variation, which is highly dependent on the reference images. This approach lacks flexibility in multi-attribute control. The face features contain all the information of faces, so Vec2Face is designed to learn face generation purely from the given face features. The advantage is that, once the model learns how to draw the target image with the given feature, the output can be easily controlled to add desired information to the vector (*i.e.*, adjusting the values).

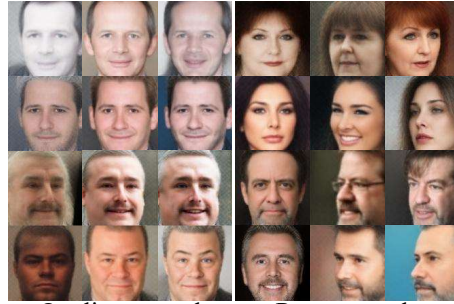
---

**Algorithm 1:** AttrOP

---

```
1 Function AttrOP ( $v_{id}, v_{im}, M_{gen}, T$ ):  
   Input: a)  $v_{id}$ : sampled ID vectors,  
           b)  $v_{im}$ : initial perturbed ID vectors,  
           c)  $M_{gen}$ : Vec2Face model,  
           d)  $T$ : the number of iterations  
   Required: target quality  $Q$ , target pose  $P$   
   Output: a)  $v'_{im}$ : adjusted perturbed ID vectors  
2   Condition models:  $M_{pose}, M_{quality}, M_{FR}$   
3   Initialization  $v'_{im} = v_{im}$   
4   for  $t = T - 1, T - 2, \dots, 0$  do  
5      $IM = M_{gen}(v'_{im})$   
6     Calculate  $\mathcal{L}_{attrOP}$  in Eq. 5  
7      $v'_{im} = v'_{im} - \lambda \nabla_{v'_{im}} \mathcal{L}_{attrOP}$   
8   return  $v'_{im}$ 
```

---



Quality control      Pose control  
Figure 4: Sample generated images after image quality control (**left**) and head pose control (**right**). For each three-image group, from left to right, image quality increases, or head poses become more profile. This improves diversity of the synthetic dataset.

**Why can Vec2Face generate images like in Fig. 1?** The FR model maps images to a hyperspherical space and clusters them. This results in, high similarity for image features from the same identity and low similarity for image features from different identities. Vec2Face learns how to generate face images based on the information in the vectors. Increasing the degree of the perturbation added to the vector gradually changes the vector direction, which results in faces from different identities.

**How can Vec2Face increase intra-class separability and inter-class variations?** A face feature vector has both identity and attribute information. Hence, controlling the cosine similarity between sampled vectors can enforce separate identities and adding small perturbations to sampled vectors could change the attributes while maintaining the identity. Moreover, AttrOP allows to more easily get the vectors to generate images with desired attributes.

**Can other structures work?** A diffusion model conditioned on image features may achieve similar function. However, the results in Appendix A.1 show that the initial noise image may exert a stronger influence on the final output than the conditioned image/identity features, which fails to preserve the identity. Our structure is image-feature-only, and the image feature is used to replace the masked-out rows in the fMAE, ensuring less noise from other factors. Thus, unless there are other special designs, our image-feature-only structure is likely to be more appropriate for this task.

**What is an identity?** An interesting philosophical question would be how to define an identity. Our research suggests that generated identities can be continuous, where a threshold  $\tau$  is used to determine the boundary between different identities. It will be interesting to study how this computational definition of identities connects with and differs from philosophical understanding in future.

## 4 EXPERIMENTS

### 4.1 DATASETS AND EVALUATION PROTOCOL

**Vec2Face training set.** The training data consists of 1M images and their features from 50K randomly sampled identities in the WebFace4M (Zhu et al., 2023) dataset, where 20 images per identity provides sufficient data for Vec2Face to learn the pattern.

**FR model training set.** The FR model for feature extraction is ArcFace-R100 trained with Glint360K (An et al., 2021) dataset. The training configurations are the same as used in the insightFace repository<sup>1</sup>.

**Real-world test sets.** The FR models are evaluated by five commonly used test sets. LFW (Huang et al., 2008) tests the FR model in a general case. CFP-FP (Sengupta et al., 2016) and CPLFW (Zheng & Deng, 2018) test the FR model on pose variation. AgeDB (Moschoglou et al., 2017) and CALFW (Zheng et al., 2017) challenge the FR model with large age gap. Besides these five, Hadrian (Wu et al., 2024a) and Eclipse (Wu et al., 2024a) are used for intra-class variation test, where

<sup>1</sup><https://github.com/deepinsight/insightface/>

Training sets	# images	LFW	CFP-FP	CPLFW	AgeDB	CALFW	Avg.
IDiff-Face (Boutros et al., 2023a) <sup>†</sup>	0.5M	98.00	85.47	80.45	86.43	90.65	88.20
DCFace (Kim et al., 2023) <sup>†</sup>	0.5M	98.55	85.33	82.62	89.70	91.60	89.56
Arc2Face (Papantoniou et al., 2024) <sup>†</sup>	0.5M	98.81	<b>91.87</b>	85.16	90.18	92.63	91.73
DigiFace (Bae et al., 2023) <sup>*</sup>	1M	95.40	87.40	78.87	76.97	78.62	83.45
SynFace (Qiu et al., 2021) <sup>◊</sup>	0.5M	91.93	75.03	70.43	61.63	74.73	74.75
SFace (Boutros et al., 2022a) <sup>◊</sup>	0.6M	91.87	73.86	73.20	71.68	77.93	77.71
IDnet (Kolf et al., 2023) <sup>◊</sup>	0.5M	92.58	75.40	74.25	63.88	79.90	79.13
ExFaceGAN (Boutros et al., 2023b) <sup>◊</sup>	0.5M	93.50	73.84	71.60	78.92	82.98	80.17
SFace2 (Boutros et al., 2024) <sup>◊</sup>	0.6M	95.60	77.11	74.60	77.37	83.40	81.62
Langevin-Disco (Geissbühler et al., 2024) <sup>◊</sup>	0.6M	96.60	73.89	74.77	80.70	87.77	82.75
<b>HSPace10K (Ours)<sup>◊</sup></b>	0.5M	<b>98.87</b>	88.97	<b>85.47</b>	<b>93.12</b>	<b>93.57</b>	<b>92.00</b>
CASIA-WebFace (Real)	0.49M	99.38	96.91	89.78	94.50	93.35	94.79

Table 1: Comparison of existing synthetic datasets on five real-world test sets. †, \*, and ◊ represent diffusion, 3D rendering, and GAN approaches, respectively, for constructing these datasets. We also list the results of training on a real-world dataset CASIA-WebFace.

Hadrian pairs emphasize facial hair difference and Eclipse pairs differ on face exposure. The images in both datasets are indoor and high quality originating from MORPH (Ricanek & Tesafaye, 2006). Ability to discriminate between similar-looking persons is tested by two datasets designed for that purpose (Deng et al., 2017; Thom et al., 2023).

**Evaluation protocol.** The image pairs in each test set are split into 10 folds. The average value of the 10-fold cross-validation is used to evaluate the model performance, as suggested in (Huang et al., 2008).

#### 4.2 EXPERIMENT DETAILS

**Vec2Face training:** We used the default ViT-Base as the backbone to form the  $MAE_f$ . Since the image size of the commonly used FR training sets is 112x112 and the image decoder is a four-layer, double-sized architecture, the feature map size is set to 49x768. After stacking the projected image features, the entire feature map becomes 50x768. The optimizer is AdamW (Loshchilov & Hutter, 2017), with a learning rate of 4e-5 and a batch size of 32 per GPU. We use approximately 10 RTX6000 GPUs for each training run. The patch-based discriminator is enabled after 1000 epochs.

**Dataset generation.** We sample separable identity vectors by PCA learned on identity vectors of MS1MV2 (Deng et al., 2019). We perturb the vectors with the noise sampled from three Gaussian distributions. Specifically, 40% from  $\mathcal{N}(0, 0.3)$ , 40% from  $\mathcal{N}(0, 0.5)$ , and 20% from  $\mathcal{N}(0, 0.7)$  for each vector. For extreme pose image generation, we generate 30 images for each identity and randomly replace the existing ones. Specifically, the target pose  $\mathcal{P}$  of 20 images is 60 and 10 images is 85. Meanwhile, we observe an image quality degradation with pure pose control, so we control the image quality with a target value 27. The iterations  $T$  is initialized as 5, but we add more conditions to the vanilla AttrOP algorithm to ensure the images have the designated attributes.

**AttrOP details.** MagFace-R100 (Meng et al., 2021) is used as the quality evaluation model, Six-DRRepNet (Hempel et al., 2024) is used as the pose evaluation model, and ArcFace-R100 is used as the identity evaluation model.

**FR dataset evaluation metric.** The quality of the synthetic datasets is evaluated by the performance of the trained model on five test sets. The standard training dataset size is 0.5M images from 10K identities. Unless otherwise specified, the backbone is SE-IR50 (He et al., 2016), the recognition loss is ArcFace (Deng et al., 2019), other configuration details are in the Appendix.

#### 4.3 MAIN EVALUATION

**Comparison with state-of-the-art synthetic datasets at the scale of 0.5M-0.6M images.** In Table 1, we compare FR accuracy of models trained with datasets synthesized by different methods such as diffusion models, GANs, and 3D rendering. We have the following observations. *First*, HSPace10K synthesized by Vec2Face yields very competitive accuracy: **98.87%**, **88.97%**, **85.47%**, **93.12%**, **93.57%** on LFW, CFP-FP, CPLFW, AgeDB, and CALFW, respectively, and **92.00%** on average. Our method is only lower than Arc2Face on the CFP-FP dataset (88.97% vs. 91.87%) and is the state of the art on all the other datasets and average. *Second*, on the CALFW dataset, the accuracy of HSPace10K is higher than, or at least competitive with that of CASIA-WebFace (Yi et al., 2014)

Methods	# images	LFW	CFP-FP	CPLFW	AgeDB	CALFW	Avg.
HSFace10K	0.5M	98.87	88.97	85.47	93.12	93.57	92.00
HSFace20K	1M	98.87	89.87	86.13	93.85	93.65	92.47
HSFace100K	5M	99.25	90.36	86.75	94.38	94.12	92.97
HSFace200K	10M	99.23	90.81	87.30	94.22	94.52	93.22
HSFace300K	15M	99.30	91.54	87.70	94.45	94.58	93.52
CASIA-WebFace (Real)	0.49M	99.38	96.91	89.78	94.50	93.35	94.79
CASIA-WebFace + HSFace10K	0.99M	<b>99.58</b>	<b>97.06</b>	<b>90.58</b>	<b>95.62</b>	<b>94.67</b>	<b>95.50</b>

Table 2: Impact of scaling the proposed HSFace dataset to 1M images (20K IDs), 5M images (100K IDs), 10M images (200K IDs), 15M images (300K IDs). Continued improvement is observed. We also list the performance obtained by training on the real-world dataset CASIA-WebFace and its combination with HSFace10K. The latter combination yields even higher accuracy.

(93.57% vs. 93.32%). To our knowledge, this is the first time that a model trained with synthetic data outperforms those trained with same-size real data. *Third*, generally speaking, GAN-based methods, while being prevalent, are not as competitive as diffusion-based and 3D rendering methods. Our method is GAN-based but has very strong performance.

**Effectiveness of scaling up the proposed HSFace dataset.** Vec2Face can easily generate a large number of distinct identity images by sampling more identity vectors which have a cosine similarity  $\leq \tau$  with any other identity vectors. Specifically, we generate 10K, 20K, 100K, 200K and 300K IDs, where each identity has 50 images. Results of models trained on these datasets are shown in Table 2.

It is clear that scaling up our synthetic dataset leads to consistent accuracy improvements: from 92.00%, to 92.47%, 92.97%, 93.22%, and 93.52%. The largest synthetic face dataset prior to this paper has 60k identities and 1.2M images (Papantoniou et al., 2024). Our dataset reaches 12.5 times larger while still giving steady improvement. These results clearly demonstrate the advantage of Vec2Face in data scaling. Also note that Vec2Face is only trained with 50K real-world identities. We speculate that a Vec2Face model trained with larger initial real data could bring about further improvements.

**Merging synthetic and real-world training sets.** In Table 2, after merging HSFace10K and CASIA-WebFace, we observe improvement over using either dataset alone for training. We obtain 95.50% average accuracy, which is higher than 92.00% (HSFace10K alone) and 94.79% (CASIA-WebFace alone). This indicates that HSFace10K has good quality and is complementary to real data.

**Effectiveness of attribute control.**

Images generated by Vec2Face are mostly near-frontal, which can be attributed to such images being most frequent in WebFace4M, the dataset used to train Vec2Face. Using AttrOP, we synthesize faces with some profile poses where we use target Yaw angles 60° and 85°. Results are shown in Table 3. We observe that adding faces with 60° poses leads to 3.46%

Attr. control	LFW	CFP-FP	CPLFW	AgeDB	CALFW	Avg.
-	98.27	76.56	81.70	90.75	92.92	88.04
+ Quality 27	98.55	83.27	83.68	91.12	93.27	89.98
+ Angle 60°	98.62	86.46	<b>85.75</b>	92.85	<b>93.80</b>	91.50
+ Angle 85°	<b>98.87</b>	<b>88.97</b>	85.47	<b>93.12</b>	93.57	<b>92.00</b>

improvement, while adding 85° gives further 0.5% improvement. These results demonstrate the effectiveness of attribute control. Note that this is achieved with Vec2Face only, instead of resorting to external models as in previous works (Kim et al., 2023; Papantoniou et al., 2024).

Table 3: Impact of face quality and pose control via AttrOP on FR performance. Each of the training sets has 0.5M images. The accuracy improvement is observed when more controls are added for image quality and pose angles, especially on pose-oriented test sets, CFP-FP and CPLFW.

**Image generation cost and quality of reconstruction.**

The resource requirement for image generation is an important metric, especially in this large model era. We compare our method with the state-of-the-art face generation model. Experimental details: 1) both models are tested on a single Titan-Xp, 2) the batch size is 8, 3) a 4-step scheduler is used for Arc2Face. Table 4 shows that our method is 311x faster than

Models	Computing cost		FID	
	Model size	FPS	LFW	Hadrian
Arc2Face	3.4GB	1.5	43.80	53.27
Vec2Face	0.68GB	467	35.75	51.93

Arc2Face. To test the quality of generated images, we use FID to measure the distance between the original LFW and Hadrian images, and the reconstructed images from Arc2Face and Vec2Face. The images are measured at 112x112 resolution. Our model slightly outperforms the Arc2Face results,

Table 4: Computing cost and FID measurement of Arc2Face (Papantoniou et al., 2024) and Vec2Face.



in size of model, speed of generation, and fidelity to original images, as shown in Table 4. The similarity measurement and examples of reconstructed images are provided in the Appendix A.1.

#### 4.4 FURTHER ANALYSIS

**Vec2Face generates datasets with large inter-class separability.** Fig. 5 presents the number of identities whose cosine similarity against any other identity vectors is less than 0.4, plotted against the number of generated identities in different datasets. A reasonable threshold varies for using different FR models (Kim et al., 2023; Boutros et al., 2024). We select 0.4 is because it gives us a reasonable number (183K out of 200K) on a real dataset. We sample 200K vectors to generate identity images by Vec2Face and Arc2Face, where we report the results of using LCM-lora (Luo et al., 2023) and DPM-solver (?) for Arc2Face. We use ArcFace-R100 to extract identity features from WebFace4M (Zhu et al., 2023) and the synthesized identity images. We have two observations.

First, synthetic datasets such as SynFace and SFace generally have lower inter-class separability than real-world datasets. This is because their data synthesis methods do not utilize the face feature characteristics for image generation, as Vec2Face and IDiff-Face do. Second, Arc2Face has much larger identity separability than existing methods, comparing with the number reported in the (Kim et al., 2023), but is still inferior to Vec2Face. This is because the initial noise image sometimes exerts a stronger influence on the final output than the conditioned identity vector. Third, real-world datasets have slightly lower identity separability than our method, because they have a small number of twins, close relatives, or even the same person with different character names in TV shows (Wu et al., 2024b).

**Note that 0.4 is not used to evaluate the number of actual identities in the dataset, but rather to provide a consistent measurement of identity separability across datasets.** Overall, the special design of Vec2Face ensures a high rate of transferring the similarity of sampled vectors to the similarity of generated images.

**Impact of inter-class separability on accuracy.** Table 7 summarizes how different average identity similarity or different levels of identity separability affect FR accuracy. Results indicate that higher identity separability is beneficial, which is consistent with previous finding (Boutros et al., 2023a). Moreover, we find that using a more strict  $\tau = 0.2$  does reduce a large number of sampled vectors, but it does not further benefit the performance.

**Vec2Face generates datasets with large intra-class variation.** Table 1 indicates the generated dataset has large variation on age and pose. We also test the performance on the test sets emphasized on the variation of other attributes. Hadrian and Eclipse (Wu et al., 2024a) have 6,000 image pairs for each and respectively control the variation on facial hair and face exposure. Table 6 shows that, while HSFace10k underperforms on accuracy, increasing the dataset size eventually surpasses the accuracy of the real dataset.

**Impact of hyperparameter  $\sigma$ .** In Vec2Face,  $\sigma$  directly controls intra-class variation, *i.e.*, larger  $\sigma$  means higher intra-class variation and vice versa. We test different configurations of  $\sigma$  values and its sampling %. Table 5 shows that, When increasing  $\sigma$ , FR accuracy first increases and then drops. Initially, increasing intra-class variation is beneficial because it creates some hard training samples. But if  $\sigma$  is too large, the generated face may look like a different person, degrading performance. Same for increasing the sampling % of the large  $\sigma$ . Thus we choose  $\sigma = \{0.3, 0.5, 0.7\}$  to sample  $\{40\%, 40\%, 20\%\}$  images for each identity.

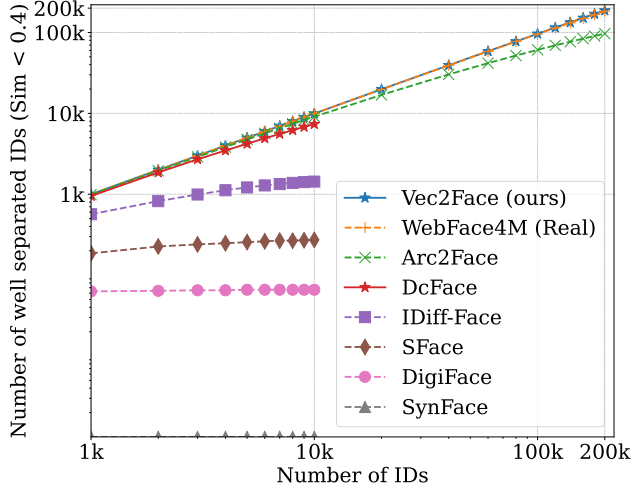


Figure 5: Inter-class separability measurement. The number of well-separated identities under different identity scales in the synthetic datasets with 10k identities, 200k generated identities from Arc2Face and Vec2Face, and real identities from WebFace4M.

$\sigma$	Sampling %	Sim <sub>min</sub>	Avg.
{0.3}	{100}	0.71	82.71
{0.3, 0.5}	{60, 40}	0.62	86.25
{0.3, 0.5, 0.7}	{40, 40, 20}	0.53	<b>88.04</b>
{0.3, 0.5, 0.7}	{20, 40, 40}	0.51	87.26
{0.3, 0.5, 0.9}	{40, 40, 20}	0.47	85.75

Table 5: Impact of  $\sigma$  values with corresponding sampling % for each identity on average FR accuracy (%). We use 0.5M images from 10K identities for training. AttrOP is not applied and Sim<sub>min</sub> is the minimum cosine similarity between the perturbed vectors and their ID vectors.

$\tau$	Avg. ID sim.	Avg.
0.3	0.88	64.62
	0.70	77.65
	0.56	78.67
	0.01	<b>88.04</b>
0.2	0.003	86.60

Table 7: Impact of inter-class separability. Larger average identity similarity (low separability) reduces the accuracy. We use 0.5M images from 10k identities for training.

Datasets	Hadrian	Eclipse	SLLFW	DoppelVer
HSFace10k	69.47	64.55	92.87	86.91
HSFace20k	75.22	67.55	94.37	88.90
HSFace100k	80.00	70.35	95.58	90.39
HSFace200k	<b>79.85</b>	<b>71.12</b>	95.70	89.86
HSFace300k	<b>81.55</b>	<b>71.35</b>	95.95	90.49
CASIA-WebFace	77.82	68.52	<b>96.95</b>	<b>95.11</b>

Table 6: Evaluation on other tasks. Hadrian, Eclipse, SLLFW, and DoppelVer emphasize facial hair variation, face exposure difference, similar-looking, and doppelganger tasks.

# IDs × # IMs	Avg.	Architecture	Avg.
10k×5	75.02	SE-IResNet18	89.60
10k×10	83.09	SE-IResNet50	92.00
10k×20	89.45	SE-IResNet100	92.49
10k×50	92.00	SE-IResNet200	92.49
10k×80	92.03	ViT-S	88.54
		ViT-B	90.15

Table 8: Impact of number of images per identity. Different number of images are generated by the best  $\sigma$  and their sampling % setting. Average accuracy (%) is reported.

Table 9: HSFace10k training on ResNets and Vision Transformers. The average accuracy (%) is reported.

**Does Vec2Face generate new identities compared with its training identities?** We compute the feature similarity between the 300k identities from the proposed synthetic data and the 50k training identities selected from WebFace4M. We find that only 0.006%, or 168 out of the 300K synthetic identities are similar to the training identities, with a similarity score greater than 0.4. To completely avoid using real identities for training FR models, we have removed these 168 identities from HSFace300K, and the performance change is negligible.

**More images per identity is beneficial.** In Table 8, increasing the number of images per identity from 5 to 80 increases the accuracy. The improvement is gradually saturated.

**Larger backbone helps the model performance.** In Table 9, accuracy of four models trained with HSFace10K and ArcFace loss increases from SE-IResNet18 to SE-IResNet100 and is saturated at SE-IResNet200. It is also useful for training with Vision Transformer (Dosovitskiy, 2020) backbones.

**Limitations.** The proposed synthetic dataset is effective for general FR but would be much less useful for fine-grained tasks such as discriminating between doppelgangers. See Table 6. We believe a better understanding of ‘identity’ and stronger generation models will help solve this issue and leave this to future work.

## 5 CONCLUSIONS

This paper proposes Vec2Face, a face generation method which can elegantly create a large number of identities and face images. This method conveniently converts vectors to face images and can translate perturbations of the vectors into consistent perturbations of the resulting face images. Because of its unique design, the inter-class and intra-class variations of generated face images can be directly controlled by hyperparameters in Vec2Face. We show that the resulting dataset, HSFace10k, has large intra- and inter-class variations and yields state-of-the-art FR accuracy. Importantly, Vec2Face allows for scaling HSFace to 300K identities and 15M images while still seeing accuracy improvement. In future work, we will study the definition of identity to solve more challenging FR tasks, try other generation structures, and extend this method to generic objects.

## REFERENCES

Vítor Albiero, Kai Zhang, and Kevin W Bowyer. How does gender balance in training data affect face recognition accuracy? In *IJCB*, pp. 1–10. IEEE, 2020.

- 
- Vitor Albiero, Xingyu Chen, Xi Yin, Guan Pang, and Tal Hassner. img2pose: Face alignment and detection via 6dof, face pose estimation. In *CVPR*, pp. 7617–7627, 2021.
- Xiang An, Xuhan Zhu, Yuan Gao, Yang Xiao, Yongle Zhao, Ziyong Feng, Lan Wu, Bin Qin, Ming Zhang, Debing Zhang, and Ying Fu. Partial FC: training 10 million identities on a single machine. In *ICCVW*, pp. 1445–1449, 2021.
- Gwangbin Bae, Martin de La Gorce, Tadas Baltrusaitis, Charlie Hewitt, Dong Chen, Julien P. C. Valentin, Roberto Cipolla, and Jingjing Shen. Digiface-1m: 1 million digital face images for face recognition. In *WACV*, pp. 3515–3524. IEEE, 2023.
- Fan Bao, Chongxuan Li, Yue Cao, and Jun Zhu. All are worth words: a vit backbone for score-based diffusion models. In *NeurIPS*, 2022.
- Fadi Boutros, Marco Huber, Patrick Siebke, Tim Rieber, and Naser Damer. Sface: Privacy-friendly and accurate face recognition using synthetic data. In *IJCB 2022*, pp. 1–11. IEEE, 2022a.
- Fadi Boutros, Marcel Klemm, Meiling Fang, Arjan Kuijper, and Naser Damer. Unsupervised face recognition using unlabeled synthetic data. *2023 IEEE 17th International Conference on Automatic Face and Gesture Recognition (FG)*, pp. 1–8, 2022b.
- Fadi Boutros, Jonas Henry Grebe, Arjan Kuijper, and Naser Damer. Idiff-face: Synthetic-based face recognition through fuzzy identity-conditioned diffusion model. In *ICCV*, pp. 19650–19661, 2023a.
- Fadi Boutros, Marcel Klemm, Meiling Fang, Arjan Kuijper, and Naser Damer. Exfacegan: Exploring identity directions in gan’s learned latent space for synthetic identity generation. In *IJCB*, pp. 1–10. IEEE, 2023b.
- Fadi Boutros, Marco Huber, Anh Thi Luu, Patrick Siebke, and Naser Damer. Sface2: Synthetic-based face recognition with w-space identity-driven sampling. *IEEE Transactions on Biometrics, Behavior, and Identity Science*, 2024.
- Qiong Cao, Li Shen, Weidi Xie, Omkar M. Parkhi, and Andrew Zisserman. Vggface2: A dataset for recognising faces across pose and age. In *IEEE F&G*, pp. 67–74, 2018.
- Li Chen, Mengyi Zhao, Yiheng Liu, Mingxu Ding, Yangyang Song, Shizun Wang, Xu Wang, Hao Yang, Jing Liu, Kang Du, et al. Photoverse: Tuning-free image customization with text-to-image diffusion models. *arXiv preprint arXiv:2309.05793*, 2023.
- Jooyoung Choi, Sungwon Kim, Yonghyun Jeong, Youngjune Gwon, and Sungroh Yoon. Hvr: Conditioning method for denoising diffusion probabilistic models. *ICCV*, 2021.
- Jiankang Deng, Jia Guo, Niannan Xue, and Stefanos Zafeiriou. Arcface: Additive angular margin loss for deep face recognition. In *CVPR*, pp. 4690–4699, 2019.
- Jiankang Deng, Jia Guo, Jing Yang, Niannan Xue, Irene Kotsia, and Stefanos Zafeiriou. Arcface: Additive angular margin loss for deep face recognition. *TPAMI*, 44, 2022.
- Weihong Deng, Jiani Hu, Nanhai Zhang, Binghui Chen, and Jun Guo. Fine-grained face verification: Fglfw database, baselines, and human-dcmn partnership. *PR*, 66:63–73, 2017.
- Alexey Dosovitskiy. An image is worth 16x16 words: Transformers for image recognition at scale. *arXiv preprint arXiv:2010.11929*, 2020.
- Patrick Esser, Robin Rombach, and Björn Ommer. Taming transformers for high-resolution image synthesis. In *CVPR*, pp. 12873–12883, 2021.
- Shanghua Gao, Pan Zhou, Ming-Ming Cheng, and Shuicheng Yan. Masked diffusion transformer is a strong image synthesizer. In *ICCV*, pp. 23164–23173, 2023.
- David Geissbühler, Hatef Otroschi Shahreza, and Sébastien Marcel. Synthetic face datasets generation via latent space exploration from brownian identity diffusion. *arXiv preprint arXiv:2405.00228*, 2024.

- 
- Kaiming He, Xiangyu Zhang, Shaoqing Ren, and Jian Sun. Deep residual learning for image recognition. In *CVPR*, pp. 770–778, 2016.
- Kaiming He, Xinlei Chen, Saining Xie, Yanghao Li, Piotr Dollár, and Ross Girshick. Masked autoencoders are scalable vision learners. In *CVPR*, pp. 16000–16009, 2022.
- Thorsten Hempel, Ahmed A. Abdelrahman, and Ayoub Al-Hamadi. Toward robust and unconstrained full range of rotation head pose estimation. *IEEE Transactions on Image Processing*, 33:2377–2387, 2024. doi: 10.1109/TIP.2024.3378180.
- Gary B Huang, Marwan Mattar, Tamara Berg, and Eric Learned-Miller. Labeled faces in the wild: A database for studying face recognition in unconstrained environments. In *Workshop on faces in 'Real-Life' Images: detection, alignment, and recognition*, 2008.
- Phillip Isola, Jun-Yan Zhu, Tinghui Zhou, and Alexei A Efros. Image-to-image translation with conditional adversarial networks. In *CVPR*, pp. 1125–1134, 2017.
- Minchul Kim, Feng Liu, Anil K. Jain, and Xiaoming Liu. Dcfacer: Synthetic face generation with dual condition diffusion model. In *CVPR*, pp. 12715–12725. IEEE, 2023.
- Jan Niklas Kolf, Tim Rieber, Jurek Elliesen, Fadi Boutros, Arjan Kuijper, and Naser Damer. Identity-driven three-player generative adversarial network for synthetic-based face recognition. In *CVPR*, pp. 806–816, 2023.
- Tianhong Li, Huiwen Chang, Shlok Mishra, Han Zhang, Dina Katabi, and Dilip Krishnan. Mage: Masked generative encoder to unify representation learning and image synthesis. In *CVPR*, pp. 2142–2152, 2023.
- Zhen Li, Mingdeng Cao, Xintao Wang, Zhongang Qi, Ming-Ming Cheng, and Ying Shan. Photomaker: Customizing realistic human photos via stacked id embedding. In *CVPR*, pp. 8640–8650, 2024.
- Ilya Loshchilov and Frank Hutter. Decoupled weight decay regularization. *arXiv preprint arXiv:1711.05101*, 2017.
- Simian Luo, Yiqin Tan, Suraj Patil, Daniel Gu, Patrick von Platen, Apolinário Passos, Longbo Huang, Jian Li, and Hang Zhao. Lcm-lora: A universal stable-diffusion acceleration module. *arXiv preprint arXiv:2311.05556*, 2023.
- Qiang Meng, Shichao Zhao, Zhida Huang, and Feng Zhou. Magface: A universal representation for face recognition and quality assessment. In *CVPR*, pp. 14225–14234, 2021.
- Stylianios Moschoglou, Athanasios Papaioannou, Christos Sagonas, Jiankang Deng, Irene Kotsia, and Stefanos Zafeiriou. Agedb: The first manually collected, in-the-wild age database. In *CVPRW*, pp. 1997–2005, 2017.
- Foivos Paraperas Papantoniou, Alexandros Lattas, Stylianios Moschoglou, Jiankang Deng, Bernhard Kainz, and Stefanos Zafeiriou. Arc2face: A foundation model of human faces. *arXiv preprint arXiv:2403.11641*, 2024.
- William Peebles and Saining Xie. Scalable diffusion models with transformers. In *ICCV*, pp. 4195–4205, 2023.
- Haibo Qiu, Baosheng Yu, Dihong Gong, Zhifeng Li, Wei Liu, and Dacheng Tao. Synface: Face recognition with synthetic data. In *ICCV*, pp. 10860–10870. IEEE, 2021.
- Alec Radford, Jong Wook Kim, Chris Hallacy, Aditya Ramesh, Gabriel Goh, Sandhini Agarwal, Girish Sastry, Amanda Askell, Pamela Mishkin, Jack Clark, et al. Learning transferable visual models from natural language supervision. In *ICML*, pp. 8748–8763, 2021.
- Karl Ricanek and Tamirat Tesafaye. Morph: A longitudinal image database of normal adult age-progression. In *IEEE F&G*, pp. 341–345, 2006.
- Robin Rombach, Andreas Blattmann, Dominik Lorenz, Patrick Esser, and Björn Ommer. High-resolution image synthesis with latent diffusion models. In *CVPR*, pp. 10684–10695, 2022.

- 
- Soumyadip Sengupta, Jun-Cheng Chen, Carlos Domingo Castillo, Vishal M. Patel, Rama Chellappa, and David W. Jacobs. Frontal to profile face verification in the wild. In *WACV*, pp. 1–9, 2016.
- Jaskirat Singh, Stephen Gould, and Liang Zheng. High-fidelity guided image synthesis with latent diffusion models. In *CVPR*, pp. 5997–6006. IEEE, 2023.
- Nathan Thom, Andrew DeBolt, Lyssie Brown, and Emily M Hand. Doppelver: A benchmark for face verification. In *International Symposium on Visual Computing*, pp. 431–444. Springer, 2023.
- Keyu Tian, Yi Jiang, Zehuan Yuan, Bingyue Peng, and Liwei Wang. Visual autoregressive modeling: Scalable image generation via next-scale prediction. *CVPR*, 2024.
- Dani Valevski, Danny Lumen, Yossi Matias, and Yaniv Leviathan. Face0: Instantaneously conditioning a text-to-image model on a face. In *SIGGRAPH*, pp. 1–10, 2023.
- Qixun Wang, Xu Bai, Haofan Wang, Zekui Qin, and Anthony Chen. Instantid: Zero-shot identity-preserving generation in seconds. *arXiv preprint arXiv:2401.07519*, 2024.
- Haiyu Wu and Kevin W Bowyer. What should be balanced in a” balanced” face recognition dataset. In *BMVC*, volume 1, pp. 2, 2023.
- Haiyu Wu, Sicong Tian, Aman Bhatta, Jacob Gutierrez, Grace Bezold, Genesis Argueta, Karl Ricanek Jr., Michael C. King, and Kevin W. Bowyer. What is a goldilocks face verification test set? *arXiv preprint arXiv:2405.15965*, 2024a.
- Haiyu Wu, Sicong Tian, Jacob Gutierrez, Aman Bhatta, Kağan Öztürk, and Kevin W Bowyer. Identity overlap between face recognition train/test data: Causing optimistic bias in accuracy measurement. *arXiv preprint arXiv:2405.09403*, 2024b.
- Guangxuan Xiao, Tianwei Yin, William T Freeman, Frédo Durand, and Song Han. Fastcomposer: Tuning-free multi-subject image generation with localized attention. *arXiv preprint arXiv:2305.10431*, 2023.
- Yuxuan Yan, Chi Zhang, Rui Wang, Yichao Zhou, Gege Zhang, Pei Cheng, Gang Yu, and Bin Fu. Facestudio: Put your face everywhere in seconds. *arXiv preprint arXiv:2312.02663*, 2023.
- Hu Ye, Jun Zhang, Sibao Liu, Xiao Han, and Wei Yang. Ip-adapter: Text compatible image prompt adapter for text-to-image diffusion models. *arXiv preprint arXiv:2308.06721*, 2023.
- Dong Yi, Zhen Lei, Shengcai Liao, and Stan Z Li. Learning face representation from scratch. *arXiv preprint arXiv:1411.7923*, 2014.
- Jiahui Yu, Yuanzhong Xu, Jing Yu Koh, Thang Luong, Gunjan Baid, Zirui Wang, Vijay Vasudevan, Alexander Ku, Yinfei Yang, Burcu Karagol Ayan, et al. Scaling autoregressive models for content-rich text-to-image generation. *arXiv preprint arXiv:2206.10789*, 2(3):5, 2022.
- Lvmin Zhang, Anyi Rao, and Maneesh Agrawala. Adding conditional control to text-to-image diffusion models. In *ICCV*, pp. 3836–3847, 2023.
- Richard Zhang, Phillip Isola, Alexei A Efros, Eli Shechtman, and Oliver Wang. The unreasonable effectiveness of deep features as a perceptual metric. In *CVPR*, pp. 586–595, 2018.
- Tianyue Zheng and Weihong Deng. Cross-pose lfw: A database for studying cross-pose face recognition in unconstrained environments. *Beijing University of Posts and Telecommunications, Tech. Rep*, 5(7), 2018.
- Tianyue Zheng, Weihong Deng, and Jiani Hu. Cross-age lfw: A database for studying cross-age face recognition in unconstrained environments. *arXiv preprint arXiv:1708.08197*, 2017.
- Zheng Zhu, Guan Huang, Jiankang Deng, Yun Ye, Junjie Huang, Xinze Chen, Jiagang Zhu, Tian Yang, Dalong Du, Jiwen Lu, and Jie Zhou. Webface260m: A benchmark for million-scale deep face recognition. *PAMI*, 45(2):2627–2644, 2023.

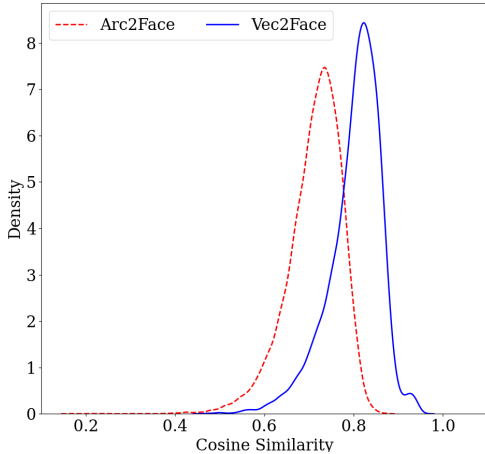


Figure 6: Similarity measurement between original and reconstructed in-the-wild images (LFW (Huang et al., 2008)).

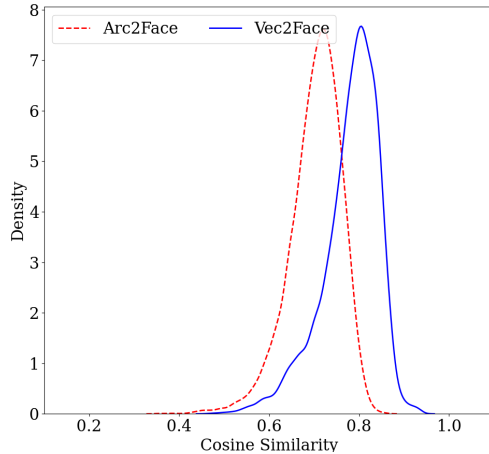


Figure 7: Similarity measurement between original and reconstructed Hadrian images (Wu et al., 2024a).

## A APPENDIX

### A.1 COMPARISON WITH DIFFUSION MODEL

Training a diffusion model conditioned with image feature vectors is a similar approach to Vec2Face. We evaluate both architectures by measuring the performance on open-set image reconstruction. The Arc2Face (Papantoniou et al., 2024) model, which fine-tuned the stable-diffusion-v1-5 on WebFace42M, is used to represent the diffusion models. The images in an in-the-wild dataset, LFW (Huang et al., 2008), and an indoor dataset, Hadrian (Wu et al., 2024a) are used for evaluation. The features are extracted by ArcFace-R100 and fed to both models. **Since both dataset are trained/fine-tuned on the cropped and aligned dataset, no image cropping and alignment are used in this evaluation.** Fig. 6 and Fig. 7 show the similarity distribution between the original images and reconstructed images. The observations are: 1) both models can preserve the identity for the in-door images, 2) Vec2Face has better performance on open-set image reconstruction on both datasets, 3) the diffusion model conditioned with image/identity features do not always preserve the identity, especially for in-the-wild images. Hence, the proposed architecture is better than the conventional diffusion model conditioned with image features. Examples are shown in Fig. 15.

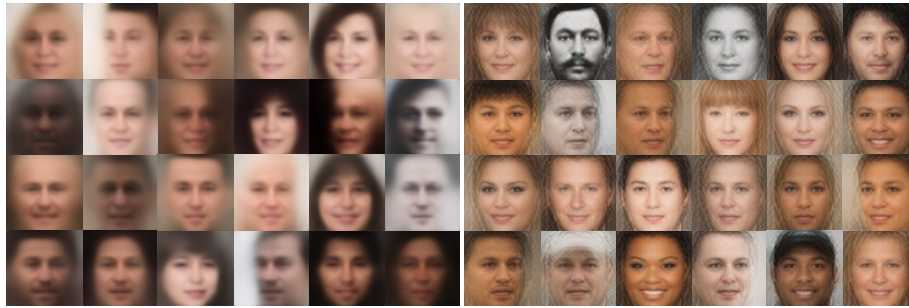
### A.2 ABLATION STUDY OF LOSS FUNCTIONS

This section presents the effects of identity loss  $L_{id}$ , perceptual loss,  $L_{lips}$  and GAN loss  $L_{GAN}$  on image reconstruction. The observations in Fig. 8 are: 1) without perceptual loss, the reconstructed face edges are smoothed, 2) involving GAN loss at an early training stage causes a glitch effect on image reconstruction, 3) without identity loss, Vec2Face performs well on near-frontal images but not on images with large pose variations.

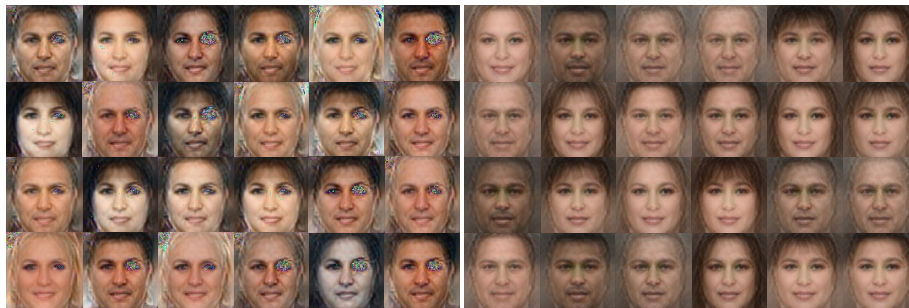
### A.3 DATASET NOISE ANALYSIS

Dataset noise could be categorized as: i) images from different identities are in the same identity folder, and ii) images from the same identity are in different identity folders. For synthetic datasets, there is no ground truth for identities, so we used the labels provided by the corresponding work.

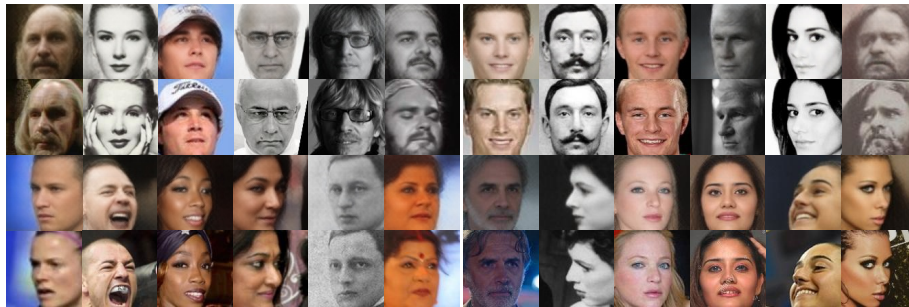
Following the metric used in previous works (Cao et al., 2018; Wu & Bowyer, 2023; Zhu et al., 2023; Deng et al., 2022), we evaluate the noise using two hard threshold values: one for the similarity between image features and their corresponding identity features, and another for the similarity across identity features. Figure 10a shows the cosine similarity distributions of the available synthetic datasets in situation one. Since greater similarity means images are more likely from the same identity, the results show that our dataset has the highest identity consistency within each identity



Effect of perceptual loss at epoch 138



Effect of GAN loss at epoch 34



Effect of identity loss

Figure 8: Examples of loss effect during training. The reconstructed examples with corresponding loss involved are on the left, otherwise on the right. For identity loss, odd rows are reconstructed images and even rows are original images.

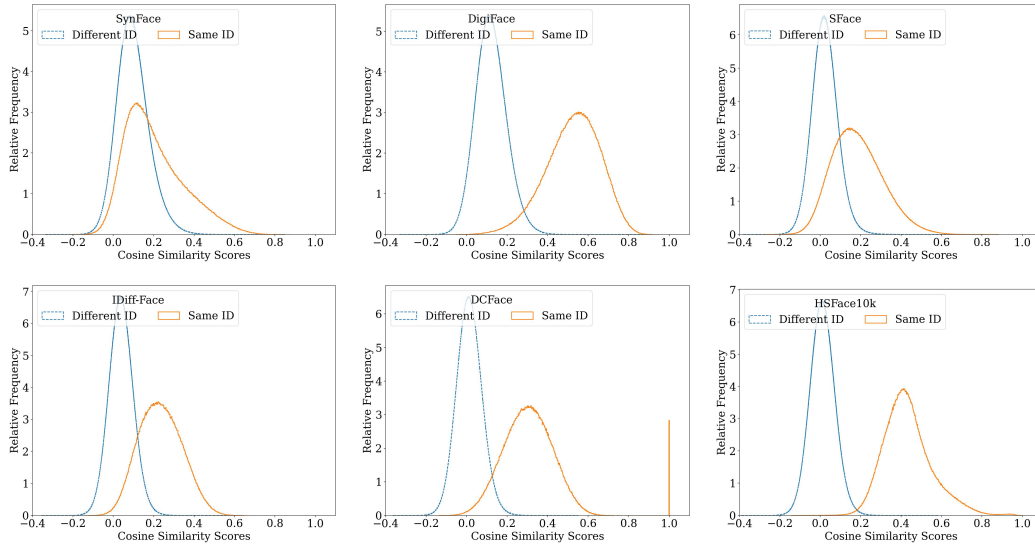
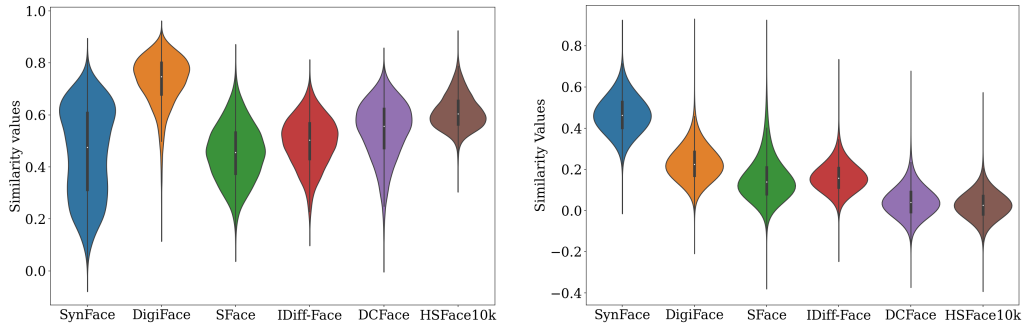


Figure 9: Similarity distributions of available synthetic datasets (Qiu et al., 2021; Boutros et al., 2022a; Bae et al., 2023; Boutros et al., 2023a; Kim et al., 2023) and ours. The results indicate that our dataset has the largest separability and smallest overlap / Equal Error Rate between genuine (**same ID**) and impostor (**different ID**) pairs.



(a) Intra-class Similarity Distributions

(b) Inter-class Similarity Distributions

Figure 10: The inter-class and intra-class similarity distributions of the available synthetic datasets (Qiu et al., 2021; Boutros et al., 2023a; Bae et al., 2023; Kim et al., 2023; Boutros et al., 2022a) and ours.

folder. Moreover, generally, if the similarity value of an image feature and its identity feature is less than 0.3, it can be regarded as an outlier/noise (Deng et al., 2022). Hence, the available synthetic datasets contain greater intra-class noise than ours. Figure 10b shows the similarity distributions of available synthetic datasets in situation two. WebFace260M (Zhu et al., 2023) is the only work discussing the details of inter-class denoising. It merged two identity folders if their identities have higher than 0.7 similarity, so if the identity similarity is larger than 0.7, we regard it as an inter-class noise. The results show that, except for DCFace and ours, the other datasets have inter-class noise to some extent.

Generally, our proposed dataset has the lowest intra-class noise and inter-class noise. Moreover, Figure 9 shows that the proposed dataset has the lowest overlapped area / Equal Error Rate (EER), showing the best dataset quality on separability between genuine (same people) and impostor (different people) pairs. It promises more reliable identity labels for the FR algorithm to learn better representations.

#### A.4 AGE AND POSE VARIATION

To estimate the distribution of age and pose, we use img2pose (Albiero et al., 2021) and an age estimator (Albiero et al., 2020) to obtain the data. Fig. 11 shows the distributions of pose and age of



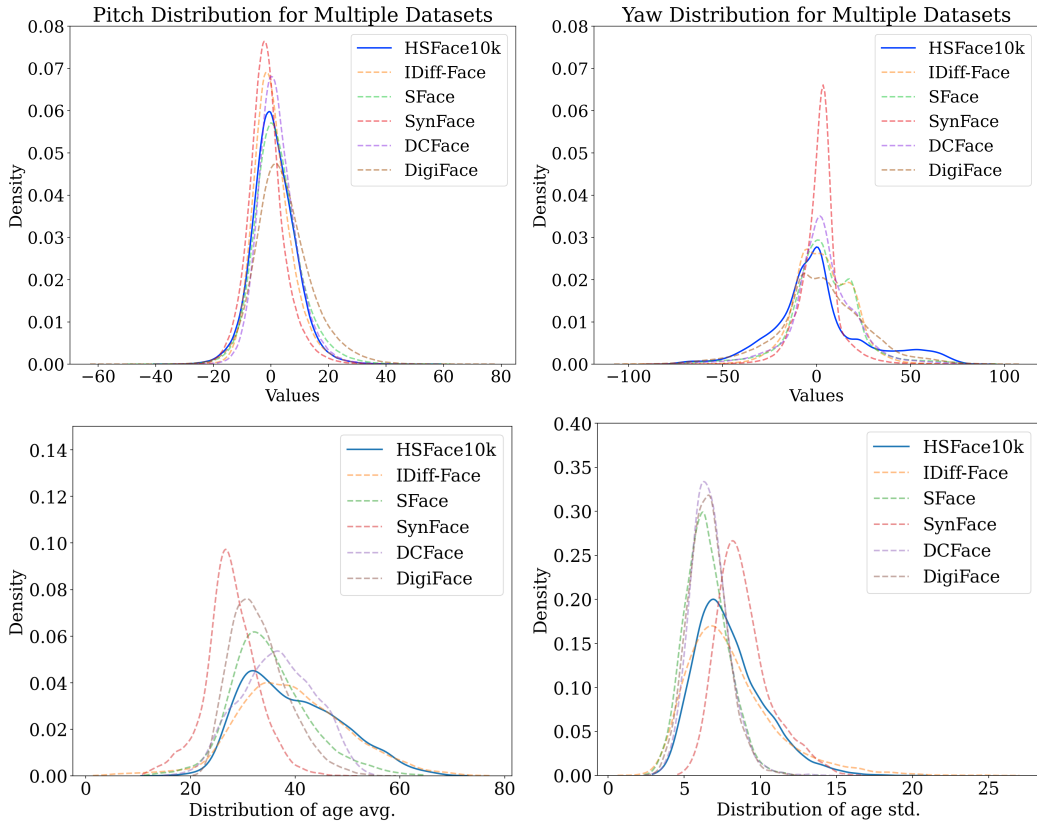


Figure 11: Pose and age variation across five test sets and HSFace10k (ours).

five available synthetic datasets and HSFace10k. Since roll is controlled by face detectors, only pitch and yaw angles are estimated. The results show that all the datasets have large variations on both pose and age, suggesting the accuracy difference is not mainly caused by the attribute variation but by identity consistency. Having large variations but losing the identity consistency results in lower accuracy.

We analyze the impact of feature values on the generated images in two ways: 1) interpolating eight feature vectors between two image features and 2) proportionally changing the values in the feature vector. Figure 12 shows the results of feature interpolation between two images. It indicates that the interpolation in the feature domain can be smoothly presented in the image domain, showcasing Vec2Face’s capability of understanding the vector characteristics in the feature domain. Figure 13 shows the results of proportionally changing the values in the feature. The observations are: 1) As the values in a feature vector increase to a large extent, the image stops changing but the quality decreases, for both negative and positive directions; 2) As the values in a feature vector become close to zero, the face attributes are erased and eventually disappear.

#### A.6 IMPACT OF VALUES AT FIXED DIMENSIONS

Vec2Face draws an image based on the values in the feature vector. We first change the values in one dimension. Fig. 16 shows the cases where some obvious patterns are observed. For each of the four identities, the value at index 15 is related to the hair volume, pose angle, age and expression; the value at index 26 have a high correlation with the bangs, facial hair and age, eyeglasses presence, and expression; increasing the value at index 32 changes the age, head pose, hair color, and expression. The observation is that changing values in a single dimension may change the face attribute but it is not consistent for all identities.

We then change the values in fixed-length (*i.e.*, 8) of dimension chunks and there are some noticeable patterns. Fig. 17 shows the generated images when the weight at specific dimensions increases. A general conclusion is that changing values at dimension chunks varies the facial attributes but the patterns are inconsistent across identities. Specifically, dimension [40:48] changes the age for the



Figure 12: Feature interpolation results. These show that Vec2Face can smoothly convert one image to another by simply changing the feature values.

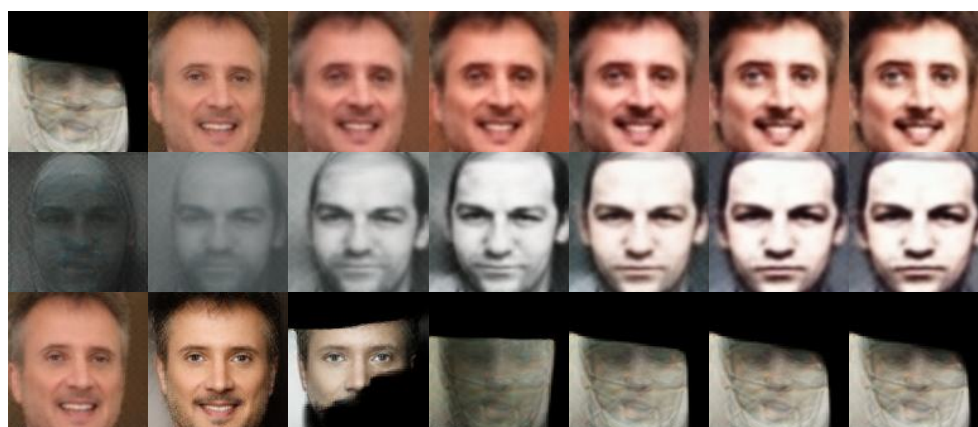


Figure 13: Impact of feature values analysis. The first row shows images generated with feature values, from left to right, of  $\{0, 1, 1.5, 2, 3, 10, 100\}$ . The second row shows images generated with feature values of  $\{-0.5, -1, -1.5, -2, -3, -10, -100\}$ . The last row shows images generated with feature values of  $\{1, 0.5, 0.25, 0.125, 0.0625, 0.03125, 0.015625\}$ .

first identity, no obvious pattern for the second, the expression for the third, and head pose for the fourth; dimension [56:64] changes the hairstyle for the first identity, facial hair for the second, age and eyeglasses for the third, age and facial hair for the fourth; dimension [96:104] changes the gender for the first identity, age and hairstyle for the second, face exposure level for the third, and facial hair for the fourth. Therefore, it is hard to control the attributes by handcrafting the features. AttrOP is much more efficient and effective.

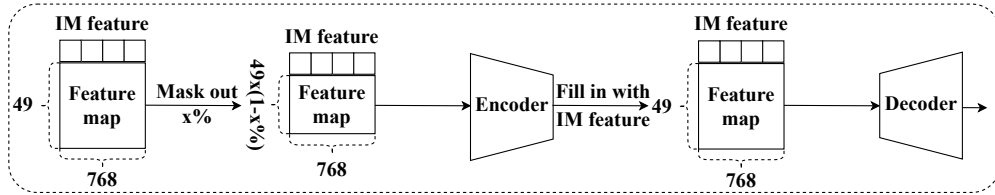


Figure 14: Architecture of the proposed feature masked autoencoder (fMAE).

Face Recognition Model Training Configurations	
Head	ArcFace
Backbone	SE-IR50
Input Size	112×112
Batch Size	128
Learning Rate	0.1
Weight Decay	5e-4
Momentum	0.9
Epochs	26
Margin	0.5
FP16	True
Sample Rate	1.0
Reduce Learning Rate	[12, 20, 24]
Augmentation	Random aug. and Random erase
Optimizer	SGD
Workers	2
GPU	RTX6000

Table 10: Configurations used for synthetic dataset training.

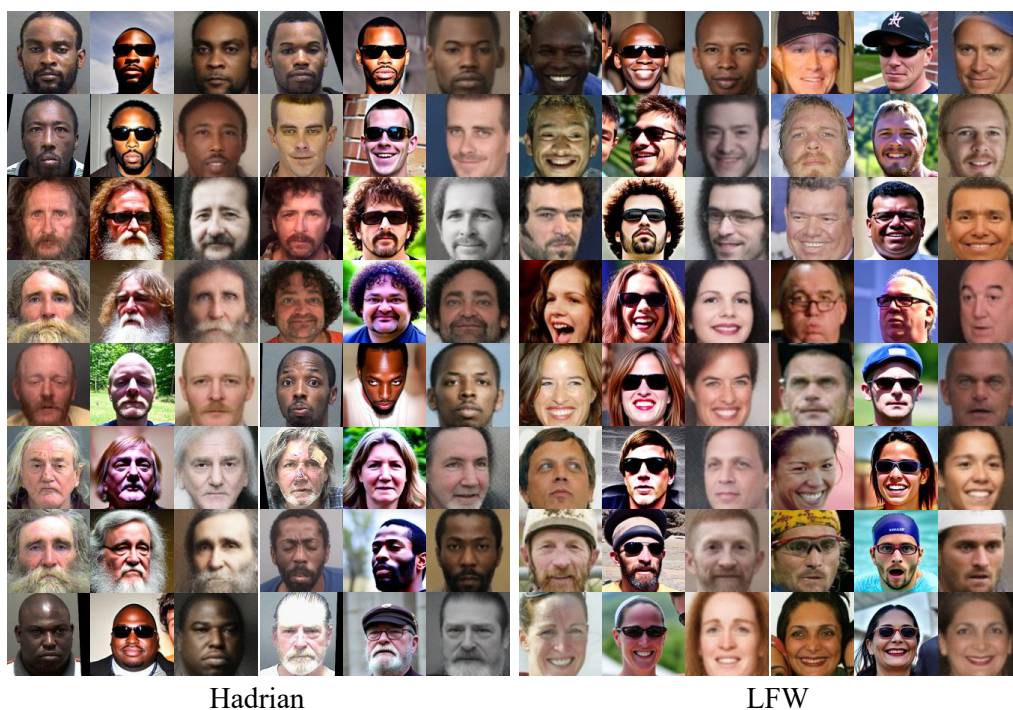


Figure 15: Examples of reconstructed Hadrian and LFW images by Arc2Face and Vec2Face. The images in each three-image group, from left to right, are the original, from Arc2Face, and from Vec2Face.



Figure 16: Examples of changing values in a single dimension. From left to right, the value gradually increases in the target dimensions. The raw images are in low quality, so we use AttrOP to increase the image quality.

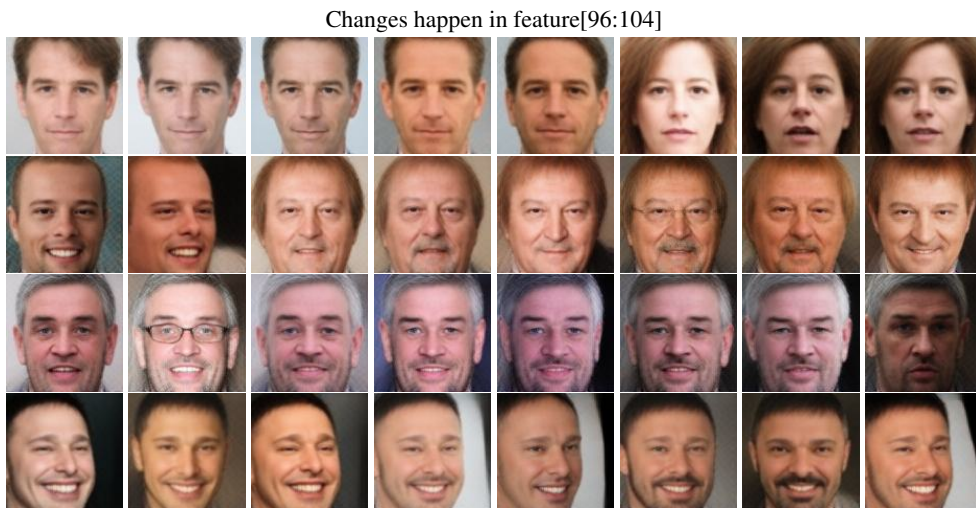
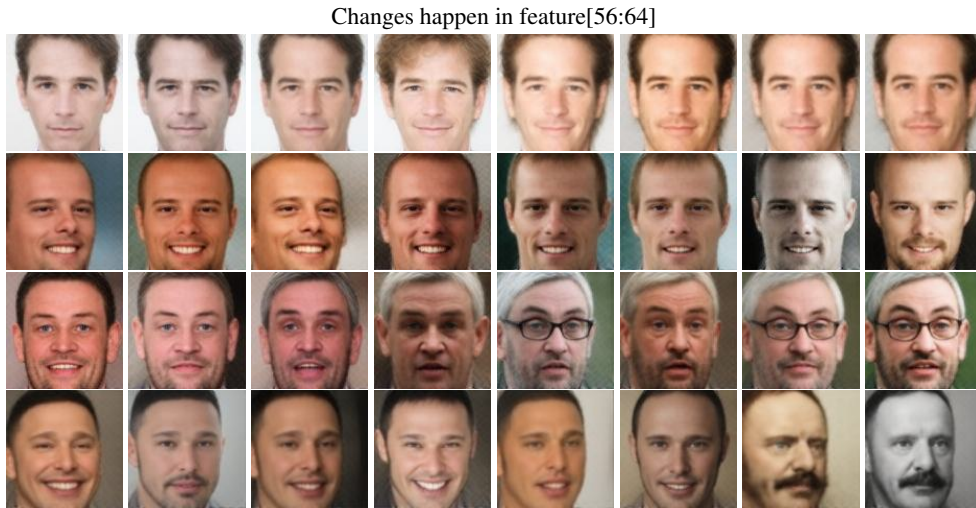
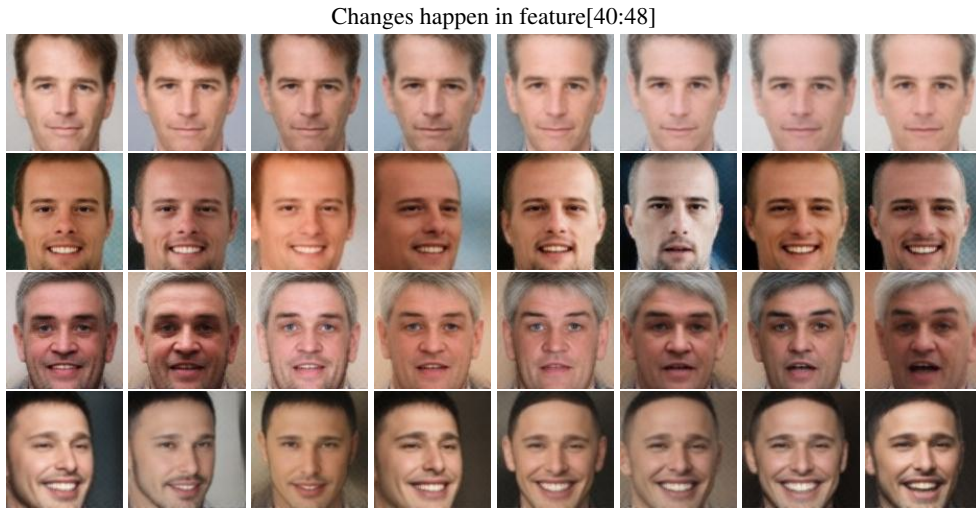


Figure 17: Examples of changing values in fixed dimensions. From left to right, the value gradually increases in the target dimensions. The raw images are in low quality, so we use AttrOP to increase the image quality.